Cell, Vol. 99, 691–702, December 23, 1999, Copyright ©1999 by Cell Press

A Role for Presenilin-1 in Nuclear Accumulation of Ire1 Fragments and Induction of the Mammalian Unfolded Protein Response

Maho Niwa,* Carmela Sidrauski,*
Randal J. Kaufman,† and Peter Walter*‡
*Howard Hughes Medical Institute and
Department of Biochemistry and Biophysics
University of California, School of Medicine
San Francisco, California 94143-0448
†Howard Hughes Medical Institute and
University of Michigan Medical Center
Ann Arbor, Michigan 48109-0650

Summary

The unfolded protein response (UPR) mediates signaling from the endoplasmic reticulum to the nucleus. In yeast, a key regulatory step in the UPR is the spliceosome-independent splicing of *HAC1* mRNA encoding a UPR-specific transcription factor, which is initiated by the transmembrane kinase/endoribonuclease Ire1. We show that yeast *HAC1* mRNA is correctly spliced in mammalian cells upon UPR induction and that mammalian Ire1 can precisely cleave both splice junctions. Surprisingly, UPR induction leads to proteolytic cleavage of Ire1, releasing fragments containing the kinase and nuclease domains that accumulate in the nucleus. Nuclear localization and UPR induction are reduced in presenilin-1 knockout cells. These results suggest that the salient features of the UPR are conserved among eukaryotic cells and that presenilin-1 controls Ire1 proteolysis in mammalian cells.

Introduction

The unfolded protein response (UPR) is an intracellular signaling pathway that connects the endoplasmic reticulum (ER) with the nucleus. Cells respond to the accumulation of unfolded proteins in the lumen of the ER by activating transcription in the nucleus of a set of genes involved in protein folding, such as the molecular chaperones BiP (or GRP78), GRP94, calreticulin, and protein disulfide isomerase. As such, the UPR adjusts the protein folding capacity of the ER according to need (reviewed by Shamu et al., 1994; Chapman et al., 1998).

UPR signaling is initiated by Ire1p, a bifunctional ER transmembrane protein with both serine/threonine kinase and endoribonuclease activities (Cox et al., 1993; Mori et al., 1993; Welihinda and Kaufman, 1996; Sidrauski and Walter, 1997). Ire1p is a single spanning ER membrane protein oriented with its N-terminal half inside the ER lumen, and its C-terminal half (which contains both the kinase and nuclease domains) in the cytosol or nucleus. The ER-lumenal portion of Ire1p is thought to function as a sensor domain that detects changes in the concentration of unfolded proteins or unbound chaperones. Activation of Ire1p leads to its phosphorylation and oligomerization, ultimately resulting in the induction of its endoribonuclease activity by unknown means (Shamu and Walter, 1996). The substrate of Ire1p is the mRNA encoding the UPR-specific transcription factor Hac1p that binds to the unfolded protein response element (UPRE) in the promoters of direct target genes of the pathway (Cox and Walter, 1996; Mori et al., 1996; Nikawa et al., 1996). Upon induction of the UPR, a 252-nucleotide intron present toward the 3′ end of *HAC1* mRNA is removed, generating the spliced form (*HAC1*^{i} mRNA, i = induced) (Cox and Walter, 1996; Kawahara et al., 1997). The first catalytic step, cleavage of *HAC1* mRNA at both intron-exon junctions, is carried out by Ire1p. The second step, ligation of the two liberated exons, is carried out by tRNA ligase, an enzyme that is shared with the pre-tRNA splicing pathway. Thus, rather than using spliceosomes, the *HAC1* intron is removed by a mechanism that resembles pre-tRNA splicing (Sidrauski et al., 1996; Gonzalez et al., 1999). Both *HAC1*^{u} mRNA (u = unspliced, uninduced) and *HAC1*^{i} mRNA are exported to the cytosol and become engaged in polyribosomes, but only the spliced form gives rise to Hac1 protein (Chapman and Walter, 1997). Splicing is therefore a key regulatory step in the UPR pathway (reviewed in Shamu, 1998; Sidrauski et al., 1998).

The recent identification of Ire1p homologs suggests that at least some aspects of the UPR are conserved in higher eukaryotic cells. In mammals, two Ire1 isoforms have been identified, Ire1α and Ire1β (Tirasophon et al., 1998; Wang et al., 1998). Overexpression of either isoform is sufficient to induce the UPR, and overexpression of dominant-negative forms blocks the pathway. Sequence comparisons show strong conservation of the C-terminal kinase and endoribonuclease domains among all known Ire1 homologs. In contrast, the ER-lumenal domains are more divergent, even between the two mammalian isoforms. The conservation of the Ire1p kinase and nuclease domains, together with the fact that human Ire1α (hIre1α) was shown to cleave the 5′ splice junction of yeast *HAC1*^{u} mRNA (Tirasophon et al., 1998), suggests that a nonconventional splicing event also plays a key role during UPR induction in higher eucaryotes. A basic leucine zipper transcription factor, ATF6, has been identified that is initially synthesized as a transmembrane protein and then becomes proteolyticlly cleaved to release a fragment that participates in transcriptional regulation upon UPR induction (Yoshida et al., 1998; Haze et al., 1999). Overexpression of a cytosolic fragment can activate transcription of UPR target genes. In contrast to yeast Hac1p, however, its mRNA is not spliced upon UPR induction.

A remaining enigma in our understanding of the UPR concerns the intracellular localization of Ire1p. From its glycosylation pattern, yeast Ire1p is known to reside in the ER membrane and/or inner nuclear membrane, which are continuous around the nuclear pores (Mori et al., 1993). The partitioning, if any, of Ire1p between these two membrane domains, i.e., whether the C-terminal domain (bearing both its kinase and nuclease functions)

‡To whom correspondence should be addressed (e-mail: pwalter@biochem.ucsf.edu).

is cytosolic or nuclear, is unknown. It is possible, however, that splicing of *HAC1* mRNA is a nuclear event because tRNA ligase is localized to the nucleus (Clark and Abelson, 1987). Thus, if the C-terminal half of Ire1p is in the cytosol, then activated Ire1p molecules must somehow enter the nucleus to participate in splicing. Ire1p might migrate to the nucleus after its biosynthesis or upon activation of the UPR. There is currently no precedent, however, for a membrane protein with a large cytoplasmic domain to move within the plane of the membrane through nuclear pores. Another possibility is that a fragment of Ire1p is proteolytically severed from the ER membrane upon UPR induction. This fragment could then migrate as a soluble protein into the nucleus to participate in splicing. A precedent for this latter mechanism is found in the pathways controlling sterol biosynthesis (reviewed by Brown and Goldstein, 1997) and Notch signaling (reviewed by Chan and Jan, 1998).

Here we provide experimental support for the hypothesis that the unusual features of the yeast UPR pathway are conserved. In mammalian cells, we expand upon the mechanism characterized in yeast to suggest that induction of the UPR involves proteolytic cleavage of Ire1, which allows its cytosolic domains to move into the nucleus, presumably as a prerequisite to participate in RNA splicing. Nuclear localization and induction of the UPR are reduced in cells lacking presenilin-1 (PS1), suggesting PS1 is a new component of the UPR that governs an essential proteolytic step.

Results

Mammalian Cells Can Carry out the Nonconventional Splicing of Yeast *HAC1* mRNA

No endogenous substrates of mammalian Ire1 isoforms have been identified; thus, to ask whether regulated mRNA splicing also plays a role in the mammalian UPR, we tested whether the unusual intron contained in yeast *HAC1* mRNA can be processed in mammalian cells. To this end, we transfected HeLa cells with a mammalian expression plasmid containing the yeast *HAC1* gene (Figure 1A). The UPR was induced by addition of the glycosylation inhibitor tunicamycin, and 4 hr later, cDNA was prepared by reverse transcription. cDNAs from both UPR-induced and -uninduced cells were then examined for splicing of *HAC1* RNA by PCR analysis using primers flanking the *HAC1* intron. As seen in Figure 1B (lane 2), cDNA from uninduced transfectants yielded a product of the size corresponding to unspliced *HAC1* cDNA. In contrast, cDNA from tunicamycin-treated cells produced an additional PCR product of 370 bp (Figure 1B, lane 4), the expected size for spliced *HAC1* cDNA. Neither PCR product was produced from cDNAs prepared from induced or uninduced nontransfected cells (Figure 1B, lane 1, and data not shown). DNA sequencing of the 370 bp band after cloning confirmed that it was derived from accurately spliced *HAC1* RNA. We confirmed these results by transfecting HeLa cells with a *HAC1* construct that was uniquely marked by a 3-nucleotide change in the 5′ exon (not shown). This control ascertained that *HAC1* RNA splicing indeed occurred in eukaryotic cells and was not due to fortuitous amplification of a spliced version of *HAC1* mRNA that might have contaminated the samples.

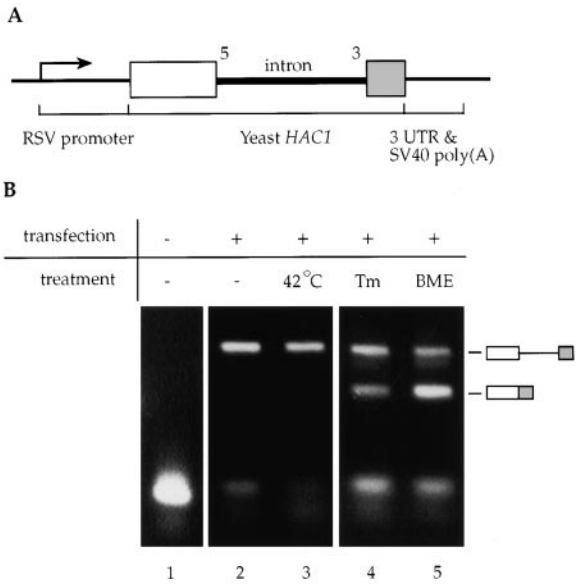

Figure 1. Yeast *HAC1* RNA Is Correctly Spliced in HeLa Cells

(A) Schematic representation of the yeast *HAC1* RNA mammalian expression vector.

(B) RT/PCR of total RNA isolated from HeLa cells 48 hr after transfection with no plasmid (lane 1) or pMH105, incubated in the absence (lane 2) or presence of tunicamycin for 2 hr (lane 4) or β-mercaptoethanol (BME) (lane 5), or heat-shocked at 42°C (lane 3). DNA was synthesized by reverse transcription and amplified by PCR using primers complementary to the 5′ and 3′ exon. Products were fractionated on agarose gels and stained with ethidium bromide. Products derived from precursor and spliced forms of yeast *HAC1* RNA are indicated.

The 370 bp band was also produced from transfectants treated with another UPR-inducing agent, the reducing agent 2-mercaptoethanol (Figure 1B, lane 5), but not from heat-shocked cells (Figure 1B, lane 3), indicating that *HAC1* mRNA splicing is dependent upon UPR induction and is not a result of general stress. Taken together, these results strongly suggest that the nonconventional splicing mechanism, which is the key step in regulation of the yeast UPR, is conserved in higher eucaryotes.

Both hIre1α and hIre1β Are Active Nucleases that Cleave the Yeast *HAC1* mRNA Intron

The strong amino acid conservation of the kinase and nuclease domain of hIre1α and hIre1β with yeast Ire1p suggests that these proteins may participate in the *HAC1* mRNA splicing reaction observed in HeLa cells. To characterize the enzymatic activities of the two human Ire1p isoforms, we expressed in baculovirus soluble His6-tagged versions of both hIre1α and hIre1β containing the kinase and nuclease domains, including the linker region between the transmembrane and kinase domains. Purification using cobalt affinity chromatography yielded major bands on SDS–PAGE of the predicted sizes of 59 kDa and 54 kDa for hIre1α(LKT) and hIre1β(LKT), respectively (Figure 2A, lanes 2 and 1, respectively).

To test for kinase activity, we incubated the purified proteins in the presence of [$\gamma-^{32}$P]ATP. Both hIre1α(LKT) and hIre1β(LKT) underwent autophosphorylation (Figure

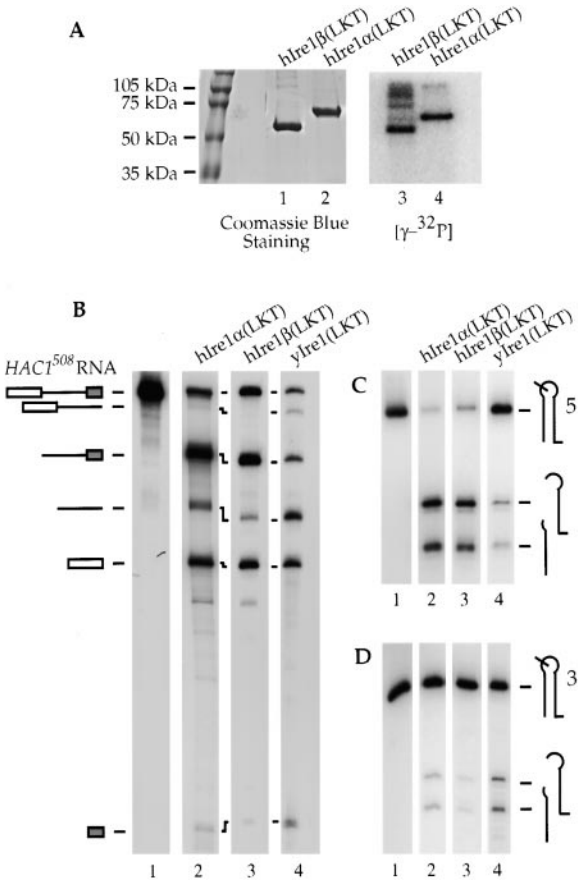

Figure 2. The Cytosolic Portions of Both hIre1α and hIre1β Have Kinase and Ribonuclease Activities In Vitro

(A) Coomassie blue staining of purified His6-tagged hIre1α(LKT) (lane 2) and hIre1β(LKT) (lane 1) after electrophoresis on an SDS-polyacrylamide gel. The in vitro kinase activities of hIre1α(LKT) (lane 4) and hIre1β(LKT) (lane 3) were tested by incubating the purified proteins with [γ−32P]ATP for 30 min at 30°C in kinase buffer.

(B) The endoribonuclease activity was tested by incubating in vitro transcribed *HAC1*^{508} RNA in the absence (lane 1) or presence of hIre1α(LKT) (lane 2), hIre1β(LKT) (lane 3), or yeast Ire1p(LKT) (lane 4) for 30 min at 30°C in kinase buffer plus 2 mM ATP. Cleavage products were separated on a 5% denaturing polyacrylamide gel. The icons indicate the different products of the cleavage reaction.

(C and D) Similarly, in vitro transcribed 5′ or 3′ splice site mini-substrates were incubated with buffer alone (lanes 1), hIre1α(LKT) (lanes 2), hIre1β(LKT) (lanes 3), or yeast Ire1p(LKT) (lanes 4).

2A, lanes 4 and 3, respectively). Quantitation indicated that under comparable conditions, hIre1α(LKT) incorporated 50-fold more phosphate than hIre1β(LKT). This difference may reflect an intrinsic difference in the respective kinase activities or could result from differences in the linker domains: the hIre1α linker region contains a serine/threonine-rich domain absent from hIre1β, and that could provide abundant phosphorylation sites. Despite this difference, our results show that both purified hIre1(LKT) isoforms are active kinases capable of autophosphorylation.

We next tested the endoribonucleolytic activity of hIre1α(LKT) and hIre1β(LKT) using a construct containing the intron and truncated 5′ and 3′ exon sequences described previously (Sidrauski and Walter, 1997). Uniformly [α-32P] UTP-labeled, in vitro transcribed yeast *HAC1*^{508} RNA was prepared and incubated in the presence of either protein. As shown in Figure 2B (lanes 2 and 3), both proteins cleaved *HAC1*^{508} RNA to produce discrete bands that are the same size as those present in a reaction containing yeast Ire1p (Figure 2B, lane 4). These observations suggest that the two hIre1 isoforms are highly specific endoribonucleases.

Recently, an efficient in vitro system utilizing mini stem–loop substrates containing either the 5′ or 3′ cleavage sites was developed that faithfully reconstitutes cleavage by yeast Ire1p (Gonzalez et al., 1999). Both hIre1(LKT) isoforms cleave the 5′ (Figure 2C, lanes 2 and 3) and the 3′ splice junction stem–loop structures (Figure 2D, lanes 2 and 3), yielding products of the same size as those obtained with yeast Ire1p (Figures 2C and 2D, lane 4). Because this assay has single nucleotide resolution, we can conclude that cleavage at both splice junctions is precise.

When comparing the efficiency of cleavage, we consistently observed that, relative to yeast Ire1p, both hIre1(LKT) isoforms cleave the 5′ splice junction more efficiently than the 3′ splice junction (compare lanes 2 and 3 in Figure 2C with lanes 2 and 3 in Figure 2D), explaining the lack of accumulation of the [5′ exon + intron] intermediate in the cleavage reaction of *HAC1*^{508} RNA (Figure 2B, lanes 2 and 3). Taken together, the data presented unambiguously show that both hIre1α(LKT) and hIre1β(LKT) are active endoribonucleases that can cleave both splice junctions of yeast *HAC1* mRNA with specificity. hIre1α(LKT) and hIre1β(LKT) are therefore strong candidates to participate in the splicing of yeast *HAC1* mRNA described above, which in turn supports the notion that a similar RNA splicing event plays a role in regulating the mammalian UPR.

Antipeptide Antibodies Distinguish hIre1α and hIre1β

The intracellular localization of yeast Ire1p is unknown, but we would expect at least some Ire1 molecules to face the nuclear compartment where they might initiate splicing of *HAC1* mRNA. We sought to determine the localization of hIre1α and hIre1β, which, owing to the larger size of mammalian cells, might be more readily detectable by immunofluorescence than in yeast, where attempts to localize endogenous Ire1p have been unsuccessful. For these studies, we raised anti-hIre1α and anti-hIre1β antibodies against peptides corresponding to unique sequences comprising the C-terminal 13 amino acids of both proteins. The immunopurified antibodies specifically recognized the cognate isoform of hIre1 as shown by Western blot analysis (Figure 3A). Each antibody reacted with the peptide (coupled to BSA) against which it was raised but not with the peptide from the other hIre1 isoform (Figure 3A, lanes 1 and 2) and recognized the correct hIre1(LKT) isoform purified from the baculovirus expression system (Figure 3A, lanes 4 and 5). Moreover, each antibody recognized a band of the expected size for full-length hIre1α and hIre1β when a blot containing a crude cell lysate was probed (Figure 3A, lanes 7 and 8). Three prominent smaller bands were also seen consistently for hIre1β. These are likely to represent proteolytic products (see below).

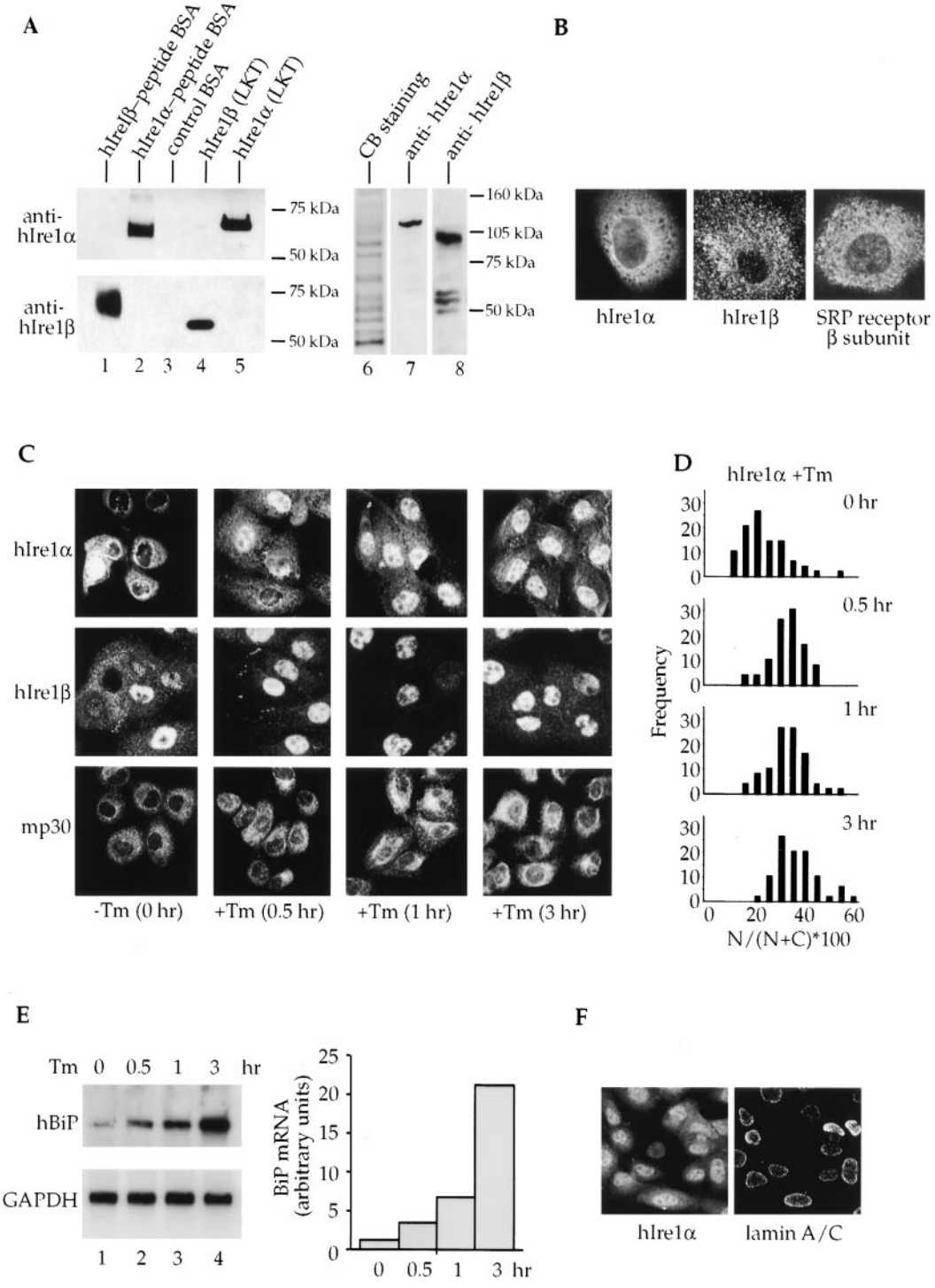

Figure 3. hIre1α and hIre1β Translocate into the Nucleus upon UPR Induction

(A) Anti-hIre1α and anti-hIre1β antibodies were tested by Western blotting against hIre1α peptide coupled to BSA (lane 2), hIre1β peptide coupled to BSA (lane 1), BSA only (lane 3), and purified His6-tagged hIre1β(LKT) and hIre1α(LKT) (lanes 4 and 5). The same antibodies were used to blot against a crude extract prepared from COS1 cells (lanes 7 and 8).

(B) COS1 cells were fixed and stained as described in Experimental Procedures. hIre1α and hIre1β were visualized by indirect immunofluorescence using immunoselected anti-hIre1α and anti-hIre1β antibodies characterized in (A) and FITC-conjugated anti-rabbit secondary antibody. An ER-localized protein, SRP receptor β subunit, was visualized similarly using an anti-SRP receptor β subunit antibody.

(C) COS1 cells were incubated with tunicamycin (Tm) for the indicated amount of time and stained for hIre1α, hIre1β, or mp30 (another ER-resident membrane protein) as described in (B).

(D) The fluorescent signals of cells stained with anti-hIre1α emanating from either the nuclear ("N") or the cytoplasmic ("C") regions of the images were integrated using a confocal microscope. The graph displays the number of cells (frequency) that fall within the specified ranges

hIre1α and hIre1β Are Localized in the ER Membrane and Are Translocated to the Nucleus upon Stimulation of the UPR

We next used the anti-peptide antibodies to localize both hIre1 isoforms in COS1 cells by indirect immunofluorescence. In most cells, staining with anti-hIre1α antibody showed a cytoplasmic staining pattern characteristic of the endoplasmic reticulum (Figure 3B, left panel). The pattern was indistinguishable from that obtained with antibodies to the β subunit of the signal recognition particle receptor and mp30 (Tajima et al., 1986), both resident ER membrane proteins (Figure 3B, right panel and Figure 3C, bottom row). In every field, a small fraction of cells (about 24%) was observed in which the nuclei were stained more brightly than the surrounding cytoplasm (Figure 3C, hIre1α, 0 hr). When cells were stained with anti-hIre1β, we consistently observed a larger number of cells (54%) in which nuclei stained more brightly than the surrounding cytoplasm (Figure 3C, hIre1β, 0 hr), whereas in a smaller number of cells the staining pattern of hIre1β was similar to that of hIre1α (Figure 3B, middle panel).

We next tested the fate of the hIre1 isoforms upon induction of the UPR. Cells were stained at three time points after addition of tunicamycin (Figure 3C). Upon UPR induction, we observed a remarkable increase in the number of cells showing nuclear staining with anti-hIre1α antibody (Figure 3C, top row). This increase was evident with 70% of the cells showing nuclear staining as early as 30 min after tunicamycin treatment. Nuclear staining was observed in nearly all cells (80%) after 1 hr and remained at that level at the 3 hr time point. Similarly, the fraction of cells that showed nuclear staining with hIre1β increased to 100% after 1 hr and remained at that level at the 3 hr time point. As expected, tunicamycin treatment did not affect the localization of the ER resident protein mp30 (Figure 3C, lower row), suggesting that the change in localization of hIre1α did not result from some gross rearrangement of the ER itself.

To estimate the amount of hIre1α undergoing relocalization, we integrated the pixel intensities of the fluorescent signal for areas of the micrographs representing cytoplasm and nucleus. The data were expressed over the time course as the percentage of the signal localized in the nucleus ($N/[N + C] \cdot 100$; N = nuclear and C = cytoplasmic). As shown in Figure 3D, the distribution of the nuclear fluorescence of hIre1α shifted significantly during UPR induction. As expected, a less pronounced shift was observed with hIre1β, as this measurement included all cells in the population and most uninduced cells already show some nuclear staining (data not shown).

Thus, it appears that a fraction of uninduced cells (a small fraction for Ire1α and a larger fraction for hIre1β) contain hIre1 in the nucleus. Superimposed on these basal levels, significant portions of both hIre1p isoforms accumulate in the nucleus upon induction of the UPR, so that virtually all cells show predominant nuclear staining. Nuclear accumulation preceded transcriptional induction of the targets of the UPR, as a significant induction of BiP mRNA was observed with a slower time course (Figure 3E).

The images shown in Figure 3 suggest that hIre1α and hIre1β in UPR-induced cells are dispersed throughout the nucleoplasm. Staining of the nucleus appears homogeneous with the nucleoli excluded (Figure 3C). Analysis of individual confocal image slices of tunicamycin-treated COS1 cells (Figure 3F, left panel) revealed no nuclear rim staining as is characteristically observed for nuclear lamins (Figure 3F, right panel). The localization suggested by these images is therefore inconsistent with that expected for integral membrane proteins.

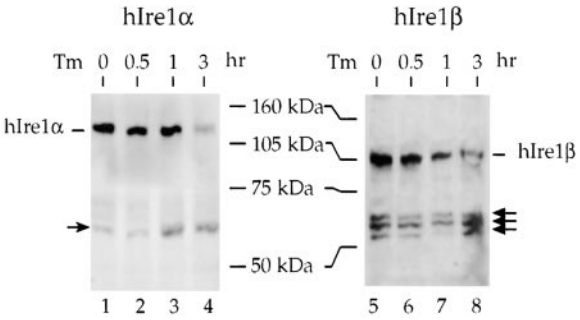

Figure 4. hIre1α and hIre1β Undergo Proteolysis during the UPR

Cells were treated with tunicamycin for the times indicated. Total cell extracts were prepared by lysing cells directly in boiling SDS buffer and probed by Western blot analysis using anti-hIre1α (lanes 1–4) and hIre1β antibodies (lanes 5–8), a biotinylated secondary antibody, and an ECL-avidin detection system.

hIre1α and hIre1β Undergo Proteolysis upon UPR Induction

One possible explanation for these results was that hIre1α and hIre1β undergo proteolysis, releasing a soluble fragment that moves into the nucleus. To test this notion, we used Western blot analysis at different time points after UPR induction to monitor the fate of the hIre1 proteins (Figure 4).

Western blots probed with anti-hIre1α antibody produced a predominant 140 kDa band in uninduced cells, consistent with the presence of full-length hIre1α, and a fainter band at approximately 60 kDa (Figure 4, lane 1). Over the time course of UPR induction, the 140 kDa band decreased with a concomitant increase of the 60 kDa band (Figure 4, lanes 2–4), suggesting that full-length hIre1α becomes proteolyzed. Based on the location of the epitope and the size of the fragment, we

of the ratio of the signal emanating from the nucleus over the total signal (N/N + C) over a time course of UPR induction with tunicamycin.

(E) COS1 cells were incubated at 37°C with tunicamycin for the indicated amount of time. Total RNA was isolated at each time point and the levels of BiP and GAPDH mRNAs were analyzed by Northern blot analysis. The data were quantitated using the PhosphorImager (Molecular Dynamics), and BiP mRNA level was normalized against GAPDH mRNA level for each lane.

(F) COS1 cells were costained with rabbit anti-hIre1α and guinea pig anti-lamin A/C antibodies using FITC- and Texas Red-conjugated secondary antibodies.

estimate that hIre1α becomes cleaved either within or just C-terminal to the transmembrane domain. The hIre1α fragment is therefore predicted to contain the linker, kinase, and nuclease domains, thus resembling the recombinant enzyme characterized above. A similar analysis using anti-hIre1β showed prominent bands of 110 kDa and three bands of around 55 kDa in uninduced cells (Figure 4, lane 5). Upon UPR induction, we observed a decrease of full-length hIre1β throughout the time course (Figure 4, lanes 6–8), but only a slight, if any, increase in the smaller molecular weight bands.

Taken together, these data suggest that UPR induction stimulates proteolytic cleavage of ER membrane-bound hIre1α and hIre1β, releasing C-terminal fragments that then migrate into the nucleus. Since both nuclear staining and smaller bands seen on Western blots are present in a significant fraction of uninduced cells, it seems likely that a UPR-independent cleavage mechanism operates normally at a reduced level in a small fraction of cells for hIre1α and in a larger fraction of cells for hIre1β.

PS1 Is Required for hIre1α and hIre1β Translocation to the Nucleus upon UPR Induction

The localization of hIre1α and hIre1β to the ER membrane raises the possibility that the protease(s) responsible for cleavage may also localize to the ER. To date, only a few ER-localized proteases have been described. Two of these are the proteases (S1P and S2P) that cleave the sterol response element–binding protein (SREBP) (Sakai et al., 1996, 1998; Rawson et al., 1997). S1P cleaves SREBP first within the ER-lumenal domain, and S2P then releases a cytosolic domain of SREBP by cleaving within its transmembrane domain. The liberated SREBP fragment then moves into the nucleus where it activates transcription. Because hIre1 cytosolic fragments appear to be similarly released, we asked whether S2P might play a role in this cleavage reaction. To this end, we monitored the localization of hIre1α and hIre1β upon UPR induction in mutant CHO cells lacking S2P protease activity due to a mutation in the S2P gene (Hasan et al., 1994; Rawson et al., 1997). In S2P mutant cells, the majority of hIre1α underwent nuclear migration upon UPR activation, whereas hIre1β was mostly localized to the nucleus prior to induction of the pathway (compare Figures 3C and 5A). Thus, the hIre1α and hIre1β staining patterns of the S2P mutant cells resemble those of COS1 cells. These results suggest that S2P protease is not involved in UPR-induced hIre1 cleavage and concomitantly confirm the UPR-dependent nuclear localization of hIre1 in a different cell line.

Another protease that cleaves type-1 transmembrane proteins to release cytosolic fragments is γ-secretase. γ-secretase cleaves amyloid precursor protein APP, which, among other products, generates $A\beta_{42}$, a major constituent of the amyloid plaques present in Alzheimer's disease patients (reviewed by Selkoe, 1998). PS1 is encoded by a gene that when mutated causes early-onset familial Alzheimer's disease (FAD) (Rogaev et al., 1995; Sherrington et al., 1995). It either harbors γ-secretase activity itself or is intimately involved in activation of γ-secretase (Wolfe et al., 1999). To determine whether PS1 is involved in hIre1 release from the membrane, we monitored the localization of hIre1 in fibroblasts derived from PS1 homozygous knockout mice ($PS1^{-/-}$ cells) or, as a control, from their wild-type litter mates ($PS1^{+/+}$ cells) (Shen et al., 1997).

Under noninducing conditions, the distribution of both hIre1α and hIre1β in $PS1^{-/-}$ cells resembled that seen in control $PS1^{+/+}$ and COS1 cells (Figures 5B and 5C, −Tm): hIre1α localized predominantly to the ER, and only a small fraction of cells (20%) showed nuclear staining. hIre1β localized in most cells (64%) to the nucleus, thus resembling the distribution described above for COS1 cells. Remarkably, upon induction of the UPR, $PS1^{-/-}$ cells exhibited only a small change in the distribution of hIre1α (changing from 20% to 37%) (Figure 5C), whereas nuclear relocalization was efficient in the $PS1^{+/+}$ control cells (100% of cells showed nuclear staining at 1.5 hr after UPR induction). Similarly, the fraction of hIre1β cells that showed nuclear staining in $PS1^{-/-}$ cells remained largely unchanged upon UPR induction (changing from 64% to 71%), whereas that in $PS1^{+/+}$ cells increased significantly (from 61% to 95%) so that virtually all cells showed nuclear accumulation after induction. Thus, these data strongly suggest that PS1 plays an important role in the UPR-dependent nuclear localization of both hIre1α and hIre1β.

The defect in nuclear localization of hIre1α in $PS1^{-/-}$ cells is further underscored by quantitative estimation of the fraction of nuclear immunofluorescence in individual cells (Figure 5D). Prior to tunicamycin treatment, the populations of $PS1^{+/+}$ and $PS1^{-/-}$ cells displayed similar relative nuclear fluorescence for hIre1α (Figure 5D, 0 hr). Following tunicamycin treatment, the average nuclear fluorescence of $PS1^{+/+}$ cells shifted significantly (Figure 5D, 1.5 hr), whereas only a slight shift was observed in $PS1^{-/-}$ cells (Figure 5D, 1.5 hr).

As some uninduced $PS1^{-/-}$ cells localize hIre1α and most uninduced $PS1^{-/-}$ cells localize hIre1β to the nucleus, there must be an additional pathway for Ire1 localization that does not require PS1. This notion is consistent with previous results showing that $PS1^{-/-}$ cells still have some γ-secretase activity and produce residual amounts of $A\beta_{42}$ (De Strooper et al., 1998). Nevertheless, our results strongly suggest that PS1 plays a crucial role in modulating Ire1p localization upon induction of the UPR pathway.

Because the $PS1^{-/-}$ and $PS1^{+/+}$ mouse fibroblasts used in this assay showed strong background bands in the molecular weight region of the Ire1 fragment that is seen by the avidin detection system, we were unable to confirm by Western blotting that $PS1^{-/-}$ cells fail to produce UPR-induced proteolytic hIre1 fragments.

Cells Lacking PS1 Have a Compromised UPR Pathway

If proteolysis and nuclear transport of hIre1α are necessary steps for UPR signal transduction, downstream events such as induction of the UPR target genes should be impaired in $PS1^{-/-}$ cells. To test this prediction directly, we examined BiP mRNA levels in $PS1^{-/-}$ and $PS1^{+/+}$ cells by Northern blot analysis after induction of the UPR (Figure 5E). In $PS1^{+/+}$ cells, BiP mRNA normalized to the housekeeping GAPDH mRNA was significantly induced (5-fold over basal level) throughout the

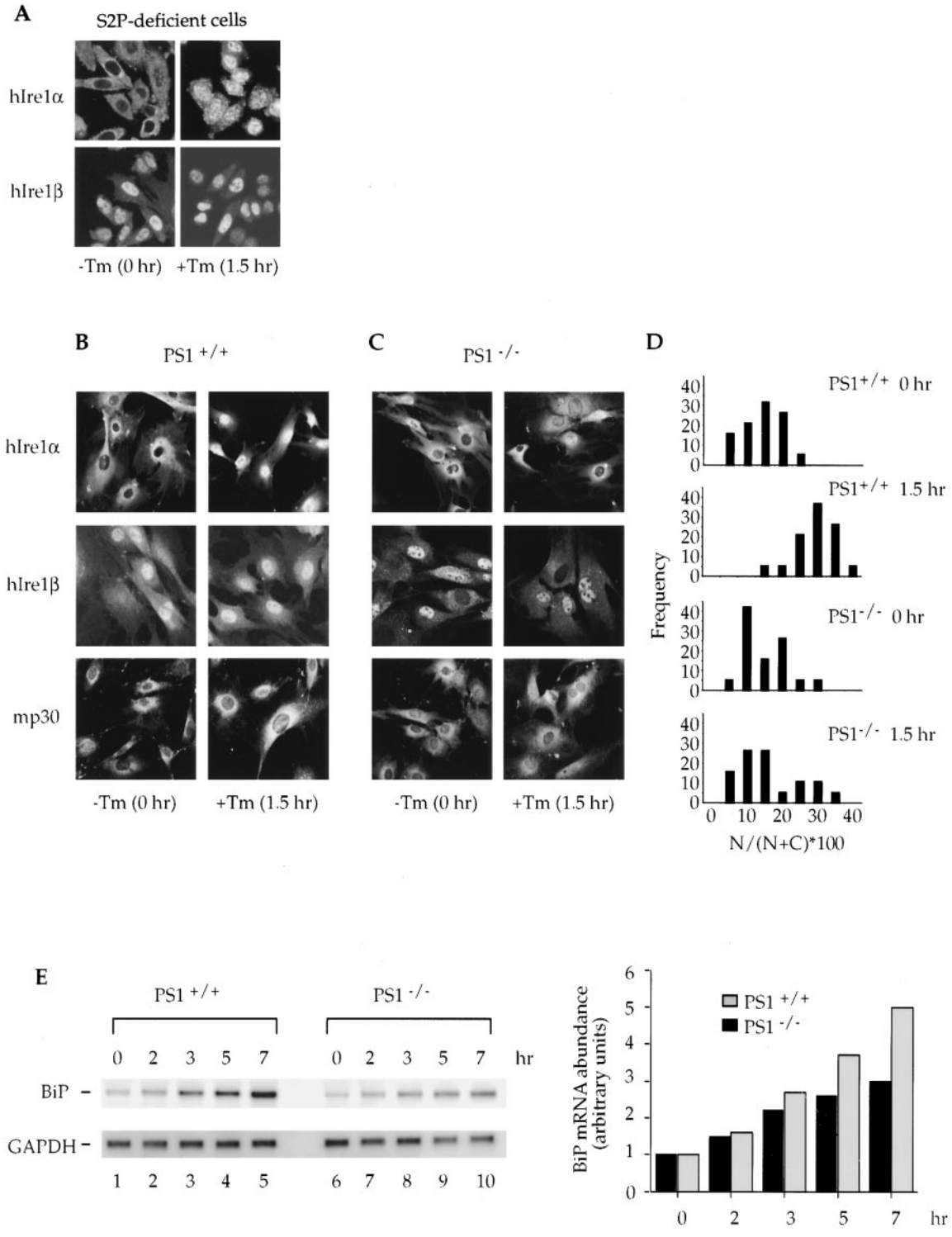

Figure 5. Nuclear Translocation of hIre1α and hIre1β upon UPR Induction Is Impaired in PS1$^{-/-}$ Cells

(A) S2P-deficient cells (M-19) were incubated in the absence (left panels) or presence (right panels) of tunicamycin for 1.5 hr. hIre1α or hIre1β was visualized by indirect immunofluorescence using either anti-hIre1α (upper panels) or hIre1β antibodies (lower panels).

(B) PS1$^{+/+}$ or (C) PS1$^{-/-}$ cells were incubated in the absence (left panels) or presence (right panels) of tunicamycin for 1.5 hr and stained with anti-hIre1α (upper panels), anti-hIre1β antibodies (middle panels), or anti-mp30 antibodies (lower panels).

(D) Quantitation of immunofluorescence was carried out as described in Figure 3.

(E) Northern analysis of BiP and GAPDH mRNAs in both PS1$^{+/+}$ (lanes 1–5) and PS1$^{-/-}$ cells (lanes 6–10), treated with tunicamycin for the indicated amount of time, was performed as described in Figure 3E.

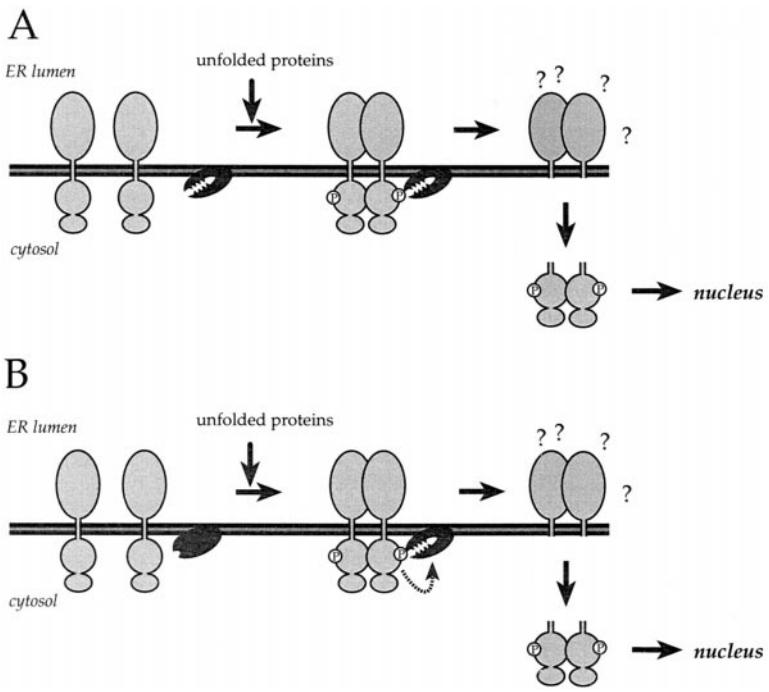

Figure 6. Model for the Activation of Mammalian Ire1 during UPR Induction

Ire1 resides on the ER membrane with its sensor domain in the lumen of the ER, where it detects accumulation of unfolded proteins via a yet unidentified mechanism. Activation of Ire1 leads to oligomerization and autophosphorylation. Ire1 is proteolytically cleaved, presumably within the transmembrane domain releasing the C-terminal cytosolic portion. Activation of Ire1 could either render Ire1 susceptible to cleavage by a constitutively active γ-secretase (pathway A) or could activate γ-secretase possibly by phosphorylation (pathway B). Other proteins might cocluster with Ire1 and be cleaved (pathway A) and/or be substrates for activated γ-secretase (pathway B). The resulting Ire1 cleavage product includes the kinase and nuclease domains and is transported into the nucleus where it may function as a site-specific endoribonuclease. The fate of the severed N-terminal domains is unknown.

7 hr time course. In contrast, BiP mRNA levels in PS1$^{-/-}$ cells increased only 3-fold over the same time period, indicating that PS1$^{-/-}$ cells can only partially activate the UPR.

Discussion

The Mammalian UPR Induces Nonconventional RNA Splicing

We have shown that some of the salient and unusual features of the yeast UPR are conserved in mammalian cells. In particular, yeast *HAC1* mRNA is correctly spliced in mammalian cells, and—as in yeast—splicing is dependent upon induction of the UPR. In addition, two human homologs of yeast Ire1p, hIre1α, and hIre1β, are now known (Tirasophon et al., 1998; Wang et al., 1998), and we have shown that both are active kinases and endoribonucleases that cleave both the 5′ and 3′ splice sites of the yeast *HAC1* mRNA with specificity (Figure 3). (In similar experiments recently performed in NIH3T3 cells, no *HAC1* mRNA splicing was detected [Foti et al., 1999]; the reason for this discrepancy is not known.) Although no mammalian homolog for Hac1p whose mRNA is subject to the nonconventional splicing reaction has yet been identified, these observations strongly suggest that the mammalian UPR is mediated by a pathway resembling that found in yeast, including a nonconventional mRNA splicing step, and predict the presence of mammalian mRNA(s) as a substrate for hIre1α and/or hIre1β. Proteins encoded by such mRNAs may be additional regulatory components that in collaboration with ATF6 induce transcription of UPR target genes.

The UPR Induces Proteolysis and Nuclear Import of Ire1 in Mammalian Cells

Superimposed on the existence of multiple isoforms of Ire1, our studies revealed additional features that have not been described for the yeast UPR. Our data on the subcellular localization and fate of hIre1α and hIre1β during UPR induction are best explained by a model (Figure 6) in which the cytosolic portions of hIre1α and hIre1β consisting of their linker, kinase, and nuclease domains are proteolytically severed from the membrane and move into the nucleus. Information from the ER lumen would be transmitted by Ire1 to alter its oligomerization and phosphorylation state and/or kinase activity, thus triggering a switch that activates the responsible proteases or renders Ire1 a substrate for constitutively active proteases (Figure 6, pathways A and B). The Ire1 fragments then move into the nucleus where they participate as endoribonucleases in mRNA splicing. This model provides a satisfying explanation of how an ER resident transmembrane protein could participate in an RNA processing event that presumably takes place in the nucleus. It is conceivable, however, that nuclear Ire1 fragments could also play other roles in addition to participating in *HAC1* splicing, including a proposed interaction with transcriptional coactivator complexes (Welihinda et al., 1997). Although proteolytic cleavage of yeast Ire1p has been proposed previously (based on the presence of a putative nuclear localization signal within the linker region of yeast Ire1p) (Mori et al., 1993), attempts to identify a proteolytic fragment of yeast Ire1p have been unsuccessful (Shamu and Walter, 1996). It thus remains to be determined whether proteolytic processing also occurs in yeast but has gone undetected or whether the processing step is an invention of higher eukaryotic cells.

Previous studies of the localization of hIre1α and mouse Ire1β reported that both proteins localized to the ER and did not detect nuclear accumulation upon UPR induction. These studies were carried out in the cells overexpressing hIre1α or mouse Ire1β (Tirasophon et al., 1998; Wang et al., 1998). It is possible that the discrepancy between these results and those reported here

lies in a limited capacity of the protease(s). Thus, most of the overexpressed hIre1 protein would remain in the ER with only a small portion of the molecules being localized in the nucleus. An intense fluorescent staining of the ER may therefore have masked a smaller signal emanating from the nucleus. Consistent with this explanation, overexpression of the cytosolic portion of Ire1β induced the UPR, yet the fragment was mostly detected in the cytosol (Wang et al., 1998). Additional problems in detecting a nuclear pool of Ire1 upon UPR induction may arise from the fact that once proteolyzed, hIre1 fragments appear to be very unstable. In our assays, detection by Western blotting required that cells be directly lysed into hot SDS-containing buffer. More conventional methods of extract preparation did not yield detectable proteolytic fragments.

We consistently observed that a fraction of uninduced cells displayed nuclear staining and, consistent with this finding, that a portion of both hIre1 isoforms was proteolyzed. We do not know why the cell population is heterogeneous in this respect or why this basal level of nuclear Ire1 accumulation is not sufficient to mount the UPR or splice yeast *HAC1* mRNA. If Ire1 is processed by different mechanisms in UPR-induced and uninduced cells, it is possible that the resulting nuclear forms differ, possibly in their oligomerization or phosphorylation states or cleavage sites, which could affect their activities. Indeed, the UPR-dependent increase in nuclear localization, but not the basal level observed in uninduced cells, is impaired by PS1 depletion. Thus, the mechanisms of nuclear hIre1 accumulation in UPR-induced and uninduced cells may be distinct.

Role of PS1 in UPR Induction and in UPR-Dependent Nuclear Localization of Ire1 Fragments

The role of PS1 in proteolytic cleavage of other transmembrane proteins prompted us to test its involvement in hIre1 proteolysis. We found that PS1$^{-/-}$ cells are reduced in their ability to mount a UPR, with a reduction in nuclear accumulation of both hIre1 isoforms. The simplest explanation for these observations is that a defect in UPR-induced proteolytic processing of Ire1 impairs its relocalization to the nucleus, thus reducing induction of the UPR. This proposal is at present a conjecture because for technical reasons, we have not yet shown directly that production of Ire1 fragments is reduced in PS1$^{-/-}$ cells. The involvement of PS1 in UPR signaling is also suggested by a concomitant independent study which shows that cells bearing PS1 mutations predisposing patients to FAD show a decreased induction of the UPR pathway as monitored by reduced BiP mRNA induction and impaired binding of factors to the UPRE (Katayama et al., 1999).

In PS1$^{-/-}$ cells, we still observe an increase in hIre1α nuclear accumulation and in BiP mRNA abundance upon UPR induction. These observations may be explained by the presence of residual γ-secretase activity in these cells (De Strooper et al., 1998), which indicates that redundant pathways exist, possibly mediated by presenilin-2, a closely related protein. Furthermore, the significant level of Ire1β always observed in uninduced or UPR-activated normal or PS1$^{-/-}$ cells was insufficient for BiP mRNA induction, suggesting that nuclear accumulation of both hIre1 isoforms may be required to induce the UPR fully.

Recently, PS1 has been also implicated in the processing of Notch, a ligand-activated transmembrane receptor involved in cell fate decisions during development (De Strooper et al., 1999; Struhl and Greenwald, 1999; Ye et al., 1999). Cleavage of Notch also occurs within the transmembrane domain, releasing the Notch intracellular domain, which activates transcription of target genes upon translocation into the nucleus. As expected, PS1$^{-/-}$ cells also show a reduced level of Notch intracellular domain (De Strooper et al., 1999). This observation has been suggested as a possible reason for the death of PS1$^{-/-}$ mice shortly after birth. Our results suggest that hIre1α and hIre1β are additional physiological substrates of PS1. The reduced ability to mount a UPR or other roles of Ire1 could be major contributing factors to the inviability of PS1$^{-/-}$ mutant mice. Thus, our results point at another potentially important function for PS1 in normal cell physiology and raise additional concerns about the potential toxicity of nonselective γ-secretase inhibitors for the treatment of Alzheimer's disease.

Possible Implications of the Link between the UPR and Alzheimer's Disease

Our results suggest that misfolding of proteins in the ER leads to increased proteolysis of Ire1 by a PS1-dependent pathway. This raises the question whether other substrates of this proteolytic system, such as APP and/or Notch, are also cleaved at an increased rate when the UPR is induced. Interestingly, it was suggested in a concurrent study that ATF6 is also synthesized as an ER transmembrane protein that becomes cleaved and enters the nucleus upon induction of the UPR (Haze et al., 1999). These observations suggest that processing of ATF6 and Ire1 could be coordinated, possibly both being carried out by γ-secretase. This putative cross-talk could be explained by either of the two pathways shown in the model in Figure 6. Ire1-dependent activation of γ-secretase might directly lead to increased processing of other substrates, including ATF6 (Figure 6, pathway B). Alternatively, activation of Ire1 might lead to the formation of protein complexes in the membrane that, in addition to Ire1, include other proteins which then also become substrates for cleavage by a constitutively active γ-secretase (Figure 6, pathway A). Thus, it is possible that APP cleavage is activated following UPR induction; ER stress may therefore lead to an increased production of $A\beta_{42}$, in turn leading to increased amyloid deposits. Environmental exposure to agents that cause ER protein misfolding or inherited mutations that predispose an individual to protein folding defects in the ER could therefore cause or accelerate the rate of onset of Alzheimer's disease. Conversely, cells bearing PS1 mutations are hypersensitive to UPR-inducing agents (Katayama et al., 1999).

In the broadest sense, it is intriguing that Alzheimer's disease involves the extracytosolic deposit of aggregated (misfolded?) $A\beta_{42}$ and that the UPR regulates the cell's extracytosolic protein folding capacity. Thus, the observation that PS1 plays a role in the UPR suggests

a potential link between a disease that results from deposits of aberrant protein and a system that monitors their proper maturation. In this light, it is particularly interesting that BiP levels are reduced in the brain of Alzheimer's disease patients. The potential connection between the UPR and the generation of amyloid deposits in Alzheimer's disease raises new possibilities for understanding and modifying the pathogenesis of this disease.

Experimental Procedures

Plasmids

The *HAC1* mammalian expression plasmid (pMH105) was constructed by cloning a 1745 bp PCR *HAC1* fragment, containing 854 nucleotides (nt) of the 5′ exon, the 252 nt intron, and 638 nt of the 3′ exon of the yeast *HAC1* gene, into the polylinker region of pRSVGEM, which is flanked by the RSV promoter and the SV40 late 3′ UTR and polyadenylation site. The baculovirus expression vector PMC10 [hIre1α(LKT)] was constructed by inserting a PCR fragment containing amino acids 469–977 of hIre1α into the EcoRI–HindII site of pFASTBacHTb (GIBCO-BRL). Similarly, PMC3 (hIre1β(LKT)) was constructed by inserting a PCR fragment containing a 463 amino acid fragment starting at the beginning of the linker domain of hIre1β into the BamHI–XhoI site of pFASTBacHTb (GIBCO-BRL).

Cell Culture and cDNA Transfection

COS1 and HeLa cells were grown in monolayer culture in Dulbecco's Modified Eagle (DME) (UCSF Cell Culture Facility) and medium supplemented with 5% and 10% fetal bovine serum (FBS), respectively, at 37°C in 5% CO_2. The PS1 knockout cell line ($PS1^{-/-}$) and the cognate wild-type cells ($PS1^{+/+}$) were kind gifts from Dr. Dennis Selkoe and were grown as described (Xia et al., 1998). M19 and CHO-K1 cells were grown as described (Hasan et al., 1994; Rawson et al., 1997).

One day prior to transfection, HeLa cells were seeded at the density of 1×10^7 cells in 100 mm dishes. Duplicated dishes were transfected with the indicated plasmids (5 μg) by either lipofection (GIBCO-BRL) or Effectine (Quiagen) in the presence of 10% FBS. Forty-eight hours after transfection, media was replaced and then tunicamycin was added to induce the UPR (10 μg/ml), and cells were further incubated for the indicated amount of time. Tunicamycin (Sigma) was dissolved in DMSO at the concentration of 10 mg/ml and diluted before use. Treatment with β-mercaptoethanol (Sigma) (15 mM) was for 4 hr, and cells were grown at 42°C for 3 hr for heat shock treatment.

Reverse Transcription and PCR

Total RNA was pretreated with DNaseI to eliminate residual genomic DNA and/or transfected plasmids. First strand cDNA was synthesized by incubating total RNA with MMTV reverse transcriptase at 37°C for 1 hr using oligo-dT as primer (GIBCO-BRL). The resulting cDNA was then subjected to PCR using primers complementary to the 5′ and 3′ exon and analyzed on a 1% agarose gel and stained with ethidium bromide. The PCR products were excised from the agarose gel and cloned using the TA cloning kit (Invitrogen, San Diego, CA). Four independent clones were sequenced.

Baculovirus Expression and Purification of hIre1α(LKT) and hIre1β(LKT)

Expression of hIre1α(LKT) and hIre1β(LKT) was performed as described in BAC-TO-BAC baculovirus expression systems (GIBCO-BRL). Insect SF-9 cells were grown in serum-free Sf-900 II SFM media at 28°C in Erlenmeyer flasks shaking at 100 rpm. The bacmid DNAs corresponding to each plasmid were transfected into Sf9 cells, and then the virus was amplified two more times (at low MOI) before infection of Sf9 cells (at high MOI) for expression. Cells were lysed in 50 mM Tris, pH 8.5, 1 mM PMSF, 1% Triton X-100, sonicated, and centrifuged at 100,000 × g. hIre1α(LKT) and hIre1β(LKT) contained N-terminal His6 tags and were purified using Pharmacia HiTrap cHeLating columns loaded with 0.2 M $CoCl_2$. The extracts were diluted in 50 mM NaPhosphate pH 8, 300 mM NaCl, and 10% glycerol (Buffer A) and bound to the column (0.5 ml/min). The column was washed extensively with Buffer A, then Buffer B (50 mM Na phosphate pH 6, 300 mM NaCl, 10% glycerol), then Buffer C (50 mM Na phosphate pH 8, 1 M NaCl, 10% glycerol), and finally Buffer A containing 20 mM immidazole. The proteins were then eluted in Buffer A containing 200 mM immidazole and buffer exchanged into kinase buffer (20 mM HEPES, pH 7.6, 1 mM DTT, 10 mM $Mg(OAc)_2$, 50 mM KOAc) plus 0.01% Nikkol and 10% glycerol. We obtained approximately 0.4 mg of each hIre1α(LKT) and hIre1β(LKT) from an 800 ml culture.

In Vitro Nuclease and Kinase Assays

In vitro transcribed [^{32}P]-labeled *HAC1^{508}* RNA, and both the 5′ and 3′ mini stem–loop substrates were prepared as described (Sidrauski and Walter, 1997; Gonzalez et al., 1999). The kinase and nuclease assays were carried out under the same conditions used for the yIre1p protein (Welihinda and Kaufman, 1996; Sidrauski and Walter, 1997; Gonzalez et al., 1999).

Northern Blot Analysis

Total cellular RNA was isolated using TRizol (GIBCO-BRL) according to the manufacturer's instructions and analyzed on 1.5% denaturing agarose gels containing 6.7% formaldehyde as described (Cox and Walter, 1996). The RNA was transferred to Duralon-UV membranes (Stratagene) and probed overnight at 42°C in hybridization buffer (50% formaldehyde, 0.2 mM NaCl, 10% dextran sulfate, 1% SDS). Probes were prepared using the Ready-to-go DNA labeling kit (Stratagene) in the presence of [α-^{32}P]dCTP. The complete coding sequence of *HAC1*, a 500 bp fragment of BiP, and a 1.2 kb GAPDH fragment were amplified by PCR and used as probes.

Anti-hIre1α and hIre1β Antibody Production

Anti-hIre1α and anti-hIre1β antibodies were raised against peptides corresponding to the 13 C-terminal amino acids. Peptides were preceded by a cysteine and were coupled to keyhole limpet hemocyanin (Sigma). Anti-hIre1α antibody was purified from the crude serum using the same peptide but coupled to Sulfo-link gel (Pierce) at the concentration of 1 mg peptide per 1 ml of gel. After loading crude serum over the peptide resin, anti-hIre1α antibodies were eluted with 1 column volume of 150 mM NaCl, 0.2 M glycine-HCl, pH 2.0, and anti-hIre1β antibodies were eluted with 6 M guanidine HCl in 0.1 M Tris-HCl, pH 8.0. Purified antibodies were precipitated with an equal volume of saturated ammonium sulfate and resuspended and stored in PBS containing 50% glycerol.

Western Blot Analysis

Cell extracts were prepared by lysing cells directly into hot SDS-containing buffer as described (Erickson and Blobel, 1979) and analyzed on either 12.5% or 8% SDS polyacrylamide gels. The Western blots were performed using the biotin/streptavidin system (Vector Laboratories, Burlingame, CA), following the manufacturer's instructions. It was necessary to use this highly amplified system; no signal was detected using more conventional enhanced chemiluminescence techniques.

Indirect Immunofluorescence Microscopy

Cells (3×10^3) were seeded on to 8-well panorama slides 12 hr prior to performing experiments. Cells were incubated with or without tunicamycin at the final concentration of 10 μg/ml for the indicated amount of time. Cells were then washed with warm PBS and fixed with 2% formaldehyde in PBS for 10 min at room temperature. Cells were blocked with PBS containing 10% fetal bovine serum, permeabilized with 0.1% saponine, and incubated with the primary antibody diluted in the blocking buffer for 1 hr at room temperature. Affinity purified anti-hIre1α and anti-hIre1β were diluted to 6 ng/ml and 2.5 ng/ml, respectively. Cells were washed three times in the blocking solution and then incubated with FITC-conjugated anti-rabbit antibody (Jackson ImmunoResearch) diluted 1:300 for additional 1 hr. Final washes were carried out with PBS without saponine. Anti-lamin A/C antibody (a kind gift from Dr. Larry Gerace) was used at the dilution of 1:2000 with rhodamine anti-guinea pig antibody

(Jackson ImmunoResearch) diluted at 1:300 as a secondary antibody. Cells were mounted in Vectashield mounting medium (Vector Laboratories).

Fluorescent Microscopy

Stained cells were viewed with a confocal DAS Microskop Leitz DMR (Leica) using either a 40× or 63× objective. Optical sections were imaged and combined in a projection with Leica TCSNT (Leica).

Quantitation of the Nuclear Fluorescent Signal

To estimate the relative nuclear fluorescence intensity, cells were costained with DAPI to demarcate the nuclear boundaries. Quantitation of the image was carried out using the Leica software by drawing outlines around the nucleus and cell periphery and integrating the pixel intensities in these areas using the projection mode of the LEICA software. The ratio of the nuclear and whole cellular fluorescence ($N/[N + C] \cdot 100$) was calculated and found to be in good agreement with the qualitative impressions of the images.

Quantitation of the Fraction of Cells with Nuclear Staining

To estimate the fraction of cells in the population that display predominant nuclear staining, fields of cells were scored using a double-blind procedure. Cells were categorized into three different classes: (1) those in which nuclei stained more intensely than the surrounding cytoplasm, (2) those that showed some intermediate nuclear staining, and (3) those in which the nuclei were unstained. Each field of cells was scored by two independent observers. Independently derived scores were in good agreement and were averaged.

Acknowledgments

We wish to express special thanks to Dennis Selkoe for the $PS1^{-/-}$ and $PS1^{+/+}$ cells, to Michael Brown and Joe Goldstein for the M19 and CHO-K1 cells, to Larry Gerace for the anti-lamin A/C antibodies. We thank Robert Rawson for providing invaluable advice in growing the M19 cells. We also thank Jason Brickner, Ursula Rüegsegger, Yu-Nang Jan, Lily Jan, and Lisa McConlogue for their helpful comments on the manuscript, and especially Ira Herskowitz, Regis Kelly, Ted Powers, and Edward Rosen for their invaluable help and support. This work was supported by postdoctoral fellowships from the Jane Coffin Childs Foundation and the American Cancer Society to M. N. and by a grant to P. W. from the National Institutes of Health. C. S. is an Associate and P. W. is an Investigator of the Howard Hughes Medical Institute.

Received October 21, 1999; revised November 23, 1999.

References

Brown, M.S., and Goldstein, J.L. (1997). The SREBP pathway: regulation of cholesterol metabolism by proteolysis of a membrane-bound transcription factor. Cell *89*, 331–340.

Chan, Y.M., and Jan, Y.N. (1998). Roles for proteolysis and trafficking in notch maturation and signal transduction. Cell *94*, 423–426.

Chapman, R.E., and Walter, P. (1997). Translational attenuation mediated by an mRNA intron. Curr. Biol. *7*, 850–859.

Chapman, R., Sidrauski, C., and Walter, P. (1998). Intracellular signaling from the endoplasmic reticulum to the nucleus. Annu. Rev. Cell Dev. Biol. *14*, 459–485.

Clark, M.W., and Abelson, J. (1987). The subnuclear localization of tRNA ligase in yeast. J. Cell Biol. *105*, 1515–1526.

Cox, J.S., and Walter, P. (1996). A novel mechanism for regulating activity of a trancription factor that controls the unfolded protein response. Cell *87*, 391–404.

Cox, J.S., Shamu, C.E., and Walter, P. (1993). Transcriptional induction of genes encoding endoplasmic reticulum resident proteins requires a transmembrane protein kinase. Cell *73*, 1197–1206.

De Strooper, B., Saftig, P., Craessaerts, K., Vanderstichele, H., Guhde, G., Annaert, W., Von Figura, K., and Van Leuven, F. (1998). Deficiency of presenilin-1 inhibits the normal cleavage of amyloid precursor protein. Nature *391*, 387–390.

De Strooper, B., Annaert, W., Cupers, P., Saftig, P., Craessaerts, K., Mumm, J.S., Schroeter, E.H., Schrijvers, V., Wolfe, M.S., Ray, W.J., et al. (1999). A presenilin-1-dependent gamma-secretase-like protease mediates release of Notch intracellular domain. Nature *398*, 518–522.

Erickson, A.H., and Blobel, G. (1979). Early events in the biosynthesis of the lysosomal enzyme Cathepsin D. J. Biol. Chem. *254*, 11771–11774.

Foti, D.M., Welihinda, A., Kaufman, R.J., and Lee, A.S. (1999). Conservation and divergence of the yeast and mammalian unfolded protein response. J. Biol. Chem. *274*, 30402–30409.

Gonzalez, T.N., Sidrauski, C., Dorfler, S., and Walter, P. (1999). Mechanism of non-spliceosomal mRNA splicing in the unfolded protein response pathway. EMBO J. *18*, 3119–3132.

Hasan, M.T., Chang, C.C., and Chang, T.Y. (1994). Somatic cell genetic and biochemical characterization of cell lines resulting from human genomic DNA transfections of Chinese hamster ovary cell mutants defective in sterol-dependent activation of sterol synthesis and LDL receptor expression. Somat. Cell Mol. Genet. *20*, 183–194.

Haze, K., Yoshida, H., Yanagi, H., Yura, T., and Mori, K. (1999). Mammalian transcription factor ATF6 is synthesized as a transmembrane protein and activated by proteolysis in response to endoplasmic reticulum stress. Mol. Biol. Cell, in press.

Katayama, T., Imaizumi, K., Sato, N., Miyoshi, K., Kudo, T., Hitomi, J., Morihara, T., Yoneda, T., Gomi, F., Mori, Y., et al. (1999). Presenilin-1 mutations downregulate the signaling pathway of the unfolded protein response. Nat. Cell Biol. *1*, 479–485.

Kawahara, T., Yanagi, H., Yura, T., and Mori, K. (1997). Endoplasmic reticulum stress-induced mRNA splicing permits synthesis of transcription factor Hac1p/Ern4p that activates the unfolded protein response. Mol. Biol. Cell *8*, 1845–1862.

Mori, K., Ma, W., Gething, M.-J., and Sambrook, J. (1993). A transmembrane protein with a cdc2+/CDC28-related kinase activity is required for signaling from the ER to the nucleus. Cell *74*, 743–756.

Mori, K., Kawahara, T., Yoshida, H., Yanagi, H., and Yura, T. (1996). Signalling from endoplasmic reticulum to nucleus: transcription factor with a basic-leucine zipper motif is required for the unfolded protein-response pathway. Genes Cells *1*, 803–817.

Nikawa, J., Akiyoshi, M., Hirata, S., and Fukuda, T. (1996). Saccharomyces cerevisiae IRE2/HAC1 is involved in IRE1-mediated KAR2 expression. Nucleic Acids Res. *24*, 4222–4226.

Rawson, R.B., Zelenski, N.G., Nijhawan, D., Ye, J., Sakai, J., Hasan, M.T., Chang, T.Y., Brown, M.S., and Goldstein, J.L. (1997). Complementation cloning of S2P, a gene encoding a putative metalloprotease required for intramembrane cleavage of SREBPs. Mol. Cell *1*, 47–57.

Rogaev, E.I., Sherrington, R., Rogaeva, E.A., Levesque, G., Ikeda, M., Liang, Y., Chi, H., Lin, C., Holman, K., Tsuda, T., et al. (1995). Familial Alzheimer's disease in kindreds with missense mutations in a gene on chromosome 1 related to the Alzheimer's disease type 3 gene. Nature *376*, 775–778.

Sakai, J., Duncan, E.A., Rawson, R.B., Hua, X., Brown, M.S., and Goldstein, J.L. (1996). Sterol-regulated release of SREBP-2 from cell membranes requires two sequential cleavages, one within a transmembrane segment. Cell *85*, 1037–1046.

Sakai, J., Rawson, R.B., Espenshade, P.J., Cheng, D., Seegmiller, A.C., Goldstein, J.L., and Brown, M.S. (1998). Molecular identification of the sterol-regulated luminal protease that cleaves SREBPs and controls lipid composition of animal cells. Mol. Cell *2*, 505–514.

Selkoe, D.J. (1998). The cell biology of beta-amyloid precursor protein and presenilin in Alzheimer's disease. Trends Cell Biol. *8*, 447–453.

Shamu, C.E. (1998). Splicing: HACking into the unfolded-protein response. Curr. Biol. *8*, R121–R123.

Shamu, C.E., and Walter, P. (1996). Oligomerization and phosphorylation of the Ire1p kinase during intracellular signaling from the endoplasmic reticulum to the nucleus. EMBO J. *15*, 3028–3039.

Shamu, C.E., Cox, J.S., and Walter, P. (1994). The unfolded-protein-response pathway in yeast. Trends Cell Biol. *4*, 56–60.

Shen, J., Bronson, R.T., Chen, D.F., Xia, W., Selkoe, D.J., and Tonegawa, S. (1997). Skeletal and CNS defects in presenilin-1 deficient mice. Cell *89*, 629–639.

Sherrington, R., Rogaev, E.I., Liang, Y., Rogaeva, E.A., Levesque, G., Ikeda, M., Chi, H., Lin, C., Li, G., Holman, K., et al. (1995). Cloning of a gene bearing missense mutations in early-onset familial Alzheimer's disease. Nature *375*, 754–760.

Sidrauski, C., and Walter, P. (1997). The transmembrane kinase Ire1p is a site-specific endonuclease that initiates mRNA splicing in the unfolded protein response. Cell *90*, 1031–1039.

Sidrauski, C., Cox, J.S., and Walter, P. (1996). tRNA ligase is required for regulated mRNA splicing in the unfolded protein response. Cell *87*, 405–413.

Sidrauski, C., Chapman, R., and Walter, P. (1998). The unfolded protein response: an intracellular signaling pathway with many surprising features. Trends Cell Biol. *8*, 245–249.

Struhl, G., and Greenwald, I. (1999). Presenilin is required for activity and nuclear access of Notch in Drosophila. Nature *398*, 522–525.

Tajima, S., Lauffer, L., Rath, V.L., and Walter, P. (1986). The signal recognition particle receptor is a complex that contains two distinct polypeptide chains. J. Cell Biol. *103*, 1167–1178.

Tirasophon, W., Welihinda, A.A., and Kaufman, R.J. (1998). A stress response pathway from the endoplasmic reticulum to the nucleus requires a novel bifunctional protein kinase/endoribonuclease (Ire1p) in mammalian cells. Genes Dev. *12*, 1812–1824.

Wang, X.Z., Harding, H.P., Zhang, Y., Jolicoeur, E.M., Kuroda, M., and Ron, D. (1998). Cloning of mammalian Ire1 reveals diversity in the ER stress responses. EMBO J. *17*, 5708–5717.

Welihinda, A.A., and Kaufman, R.J. (1996). The unfolded protein response pathway in *Saccharomyces cerevisiae*. Oligomerization and trans-autophosphorylation of Ire1p (Ern1p) are required for kinase activation. J. Biol. Chem. *271*, 18181–18187.

Welihinda, A.A., Tirasophon, W., Green, S.R., and Kaufman, R.J. (1997). Gene induction in response to unfolded protein in the endoplasmic reticulum is mediated through Ire1p kinase interaction with a transcription coactivator complex containing Ada5p. Proc. Natl. Acad. Sci. USA *94*, 4289–4294.

Wolfe, M.S., Xia, W., Ostaszewski, B.L., Diehl, T.S., Kimberly, W.T., and Selkoe, D.J. (1999). Two transmembrane aspartates in presenilin-1 required for presenilin endoproteolysis and γ-secretase activity. Nature *398*, 513–517.

Xia, W., Zhang, J., Ostaszewski, B.L., Kimberly, W.T., Seubert, P., Koo, E.H., Shen, J., and Selkoe, D.J. (1998). Presenilin 1 regulates the processing of beta-amyloid precursor protein C-terminal fragments and the generation of amyloid beta-protein in endoplasmic reticulum and Golgi. Biochemistry *37*, 16465–16471.

Ye, Y., Lukinova, N., and Fortini, M.E. (1999). Neurogenic phenotypes and altered Notch processing in Drosophila Presenilin mutants. Nature *398*, 525–529.

Yoshida, H., Haze, K., Yanagi, H., Yura, T., and Mori, K. (1998). Identification of the *cis*-acting endoplasmic reticulum stress response element responsible for transcriptional inducion of mammalian glucose-regulated proteins. J. Biol. Chem. *273*, 33741–33749.